

Recent Results of the PLUTO-Collaboration

Jochen Bürger

Siegen University, Department of Physics

D 5900 Siegen 21, Fed. Rep. of Germany

and

Deutsches Elektronen Synchrotron DESY

D 2000 Hamburg 52, Fed. Rep. of Germany



Abstract: New results obtained in e^+e^- -annihilation are presented, concerning the total hadronic cross section, the ρ -inclusive production, the radiative decay $J/\psi \rightarrow f^0\gamma$ and properties of the heavy lepton τ .

Résumé: On a présenté des nouveaux résultats qui ont été obtenus dans l'annihilation e^+e^- et qui concernent la section efficace hadronique, la production inclusive des mesons ρ , la désintégration radiative $J/\psi \rightarrow f^0\gamma$ et des propriétés du lépton lourd τ .

1. Introduction

The results of the PLUTO-collaboration* presented in this talk are based on data taken in the runperiod of 1976. In 1977 the PLUTO detector was upgraded with several new components. In the same year the DORIS-storage ring has also been upgraded to higher energies.

Thus the set of data discussed in the following is the same as described in the talk of V.Blobel held at the XII. Rencontre de Moriond⁽¹⁾ one year ago, where he gave details on the energies we run and the integrated luminosities.

My talk is organized as follows:

In chapter 2 I shall give a brief description of the PLUTO detector, chapters 3 to 5 are dealing with the total hadronic cross section, with the ρ -inclusive production and with the radiative decay $J/\psi \rightarrow f^0\gamma$, which may be compared with theoretical predictions especially from quantumchromodynamics (QCD), chapter 6 discusses new results on the heavy lepton τ . In a concluding chapter 7 a short review on the present and future programs of the PLUTO detector is given.

*at present the PLUTO-Collaboration consists of the following physicists:

Ch.Berger, W.Lackas, F.Raupach, W.Wagner, I.Physikalisches Institut
der RWTH Aachen;

G.Alexander¹, L.Criegee, H.C.Dehne, K.Derikum, R.Devenish, G.Flügge, G.Franke,
Ch.Gerke, E.Hackmack, P.Harms, G.Horlitz, Th.Kahl², G.Knies, E.Lehmann,
B.Neumann, R.L.Thompson³, U.Timm, P.Waloschek, G.G.Winter, S.Wolff, W.Zimmer-
mann, Deutsches Elektronen-Synchrotron DESY, Hamburg;

O.Achterberg, V.Blobel, L.Boesten, H.Daumann, A.F.Garfinkel⁴, H.Kapitza,
B.Koppitz, W.Lührsen, R.Maschuw, H.Spitzer, R.van Staa, G.Wetjen,
II. Institut für Experimentalphysik der Universität Hamburg;

A.Bäcker, J.Bürger, C.Grupen, H.J.Meyer, G.Zech, Siegen University;
H.J.Daum, H.Meyer, O.Meyer, M.Rössler, K.Wacker, Wuppertal University.

(¹On leave from Tel-Aviv University, Israel; ²Now at Max-Planck-Institut für
Physik und Astrophysik, München; ³On leave from Humboldt University, Arcata,
California, USA; ⁴On leave from Purdue University, W.Lafayette In., USA.)

2. Brief Description of the Detector

PLUTO is a magnetic 4π detector at the DORIS e^+e^- storage ring at DESY in Hamburg. The details of this detector are described in several publications ^(2,3), thus I shall only mention the most important features of this apparatus.

A schematic view of the PLUTO detector as used in 1976 is given in fig.1. The detector consists of a superconducting solenoid providing a magnetic field of 2 Tesla in its inner volume (1.4 m diameter and 1.1 m length), which is filled with 14 cylindrical proportional wire chambers and two cylindrical lead converters all concentric to the beam. Thus track recognition and momentum measurement for charged tracks is possible. The flux return yoke which is used simultaneously as hadron absorber, is covered with a muon detector consisting of plane proportional tube chambers. On the average a particle coming from the interaction point has to penetrate 68 cm of iron equivalent to reach the muon chambers.

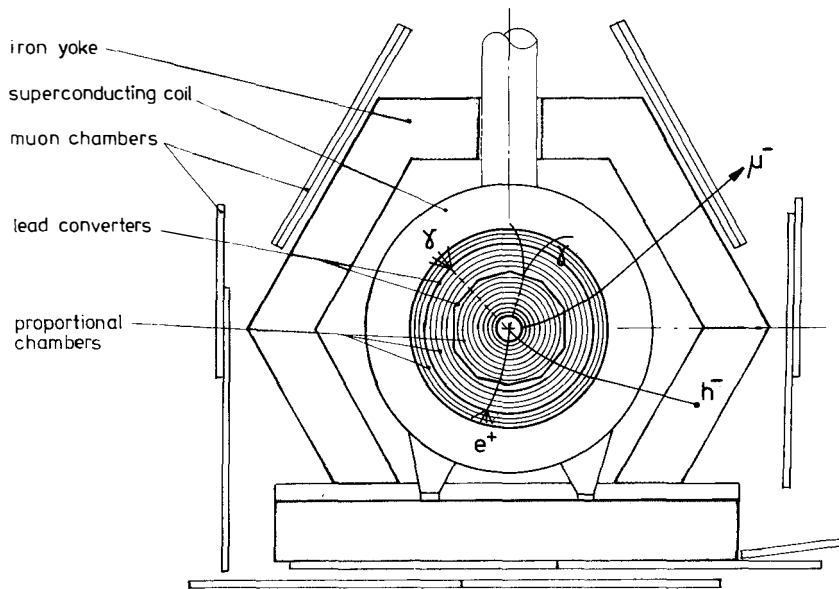


Fig.1 Schematic view of the PLUTO detector (1976) with typical particle signatures (view along the beamline)

The geometrical acceptances of the different detector components are listed in the table below.

Table 1. Solid angle coverage of detector components

Detector component	Solid angle in % of 4π
Proportional wire chambers	
- purely geometric	92
- with trigger	87
Inner lead converter ($r = 37.5$ cm) (0.44 radiation lengths thick)	78
Outer lead converter ($r = 59.5$ cm) (1.71 radiation lengths thick)	60
Muon chambers	51
- with $ \cos \theta < .55$	45

Particle identification is possible to a certain extent with this apparatus, the signatures of particles used in the context of this talk are the following:

Electrons are charged tracks giving showers behind one of the two lead converters.

Muons are non showering charged tracks which can be extrapolated from the inner detector to a muon chamber having a set wire within a certain region around the extrapolated track. Charged hadrons (mostly assumed to be pions) are all charged tracks coming from the interaction point not showering behind both lead converters. A special class of these hadrons are the "identified" ones, having sufficient energy to penetrate the iron if they were muons, and pointing towards a muon chamber which has no set wire within the appropriate region around the extrapolated track. If a photon has been converted in the second layer of lead, it can be identified by a shower in the two proportional chambers behind the lead, if this shower is not correlated with a track. In this case only the determination of the direction of the photon is possible. If the photon produces an electron-positron pair already in the first converter, also its energy can be measured.

3. Total Hadronic Cross Section

Our measurements of the total hadronic cross section have been published in an updated version at the Hamburg-Conference last summer⁽⁴⁾. Here I shall discuss these results only in a brief manner comparing them with other results.

The data used to gain our cross section include all events with ≥ 2 tracks, having at least one track with an angle against the beam axis $\theta > 30^\circ$ and a momentum $p > 240$ MeV/c. For two-prongs a coplanarity angle $15^\circ < \Delta\phi < 165^\circ$ is required. Radiative corrections have been applied to the measured cross section. To determine all acceptances a Monte Carlo procedure was used, which simulates as exact as possible all details of the detector. The data are best described, if the physical model fed into this Monte Carlo procedure is of the "jet" type, with a jet-axis distribution proportional to $(1 + \cos^2 \theta)$ and an average transverse momentum with respect to the jet-axis of $\langle p_t \rangle = 350$ MeV/c⁽⁵⁾.

The overall efficiency and acceptance is for two-prongs $\sim 40\%$ and for >2 -prongs $\sim 95\%$ giving a total efficiency of $\sim 75\%$ for all events. Due to these high efficiencies the Monte Carlo corrections applied to our data are relatively small compared to other detectors.

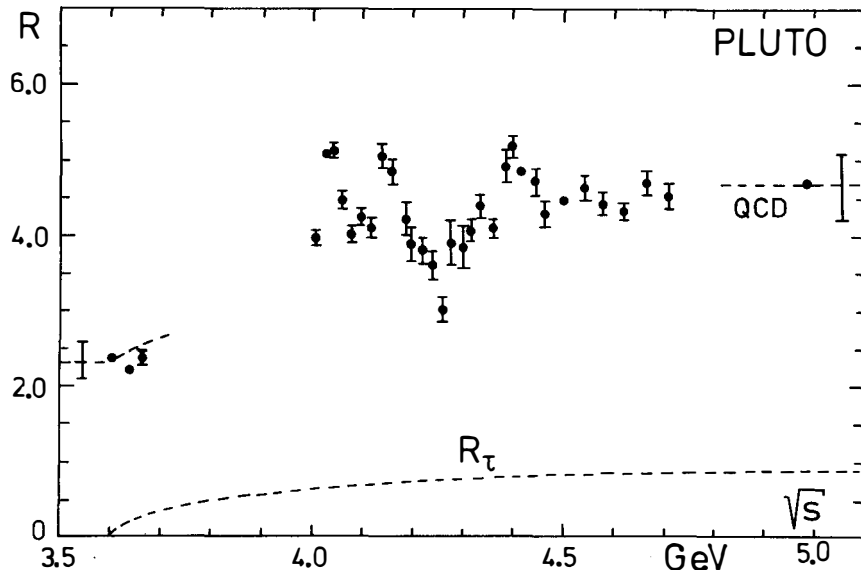


Fig. 2 Total hadronic cross section $R_{\text{tot}} = \sigma_{\text{had}} / \sigma_{\mu\mu}$
(contribution from the heavy lepton τ included)

In fig.2 the ratio

$$R_{\text{tot}} = \sigma(e^+e^- \rightarrow \text{hadrons}) / \sigma(e^+e^- \rightarrow \mu^+\mu^-)$$

is plotted as a function of the center of mass energy \sqrt{s} .

In the framework of quantumchromodynamics (QCD) the total hadronic cross section (without the contribution from the heavy lepton τ) including the first order gluonic corrections is given by

$$R_{\text{had}} = 3 \sum_i Q_i^2 \cdot (1 + \alpha_s/\pi)$$

where Q_i are the quark charges ($i = u, d, s$ for $\sqrt{s} < 3.6$ GeV and $i = u, d, c, s$ for $\sqrt{s} > 3.6$ GeV) and α_s the running coupling constant of the strong interactions:

$$\alpha_s = \frac{12\pi}{(33-2n)\ln(s/\Lambda^2)}$$

($n = \text{number of quark flavours}$)

The only free parameter is Λ . A fit to deep inelastic lepton-nucleon scattering data yields a value of $\Lambda \sim 0.5$ GeV, which will be used in this estimation. For $\sqrt{s} = 3.6$ GeV this leads to a value of $R_{\text{had}} = R_{\text{tot}} = 2.2$ and for $\sqrt{s} = 5.0$ GeV to $R_{\text{had}} = 3.7$. But these corrections are far too small to be measured with existing detectors. To obtain at the latter energy the value of R_{tot} one must add the contribution of the threshold factor of the heavy lepton τ

$$R_{\tau} = (3\beta - \beta^3)/2 \quad (\beta = \text{velocity of the } \tau)$$

At $\sqrt{s} = 5$ GeV one has $R_{\tau} = .98$ yielding for $R_{\text{tot}} = 4.7$, because all $\tau^+\tau^-$ -events contribute to the hadronic events selected. For both values at 3.6 GeV below and at 5.0 GeV above charm - and heavy lepton - thresholds the measured R_{tot} is in good agreement with theoretical expectations, but one must always keep in mind that an overall systematic uncertainty of about 10% must be taken into account, which is on top of the gluonic corrections.

The topology of the cross section shows three distinct peaks. The results of separate fits to each of these resonance like regions are given in table 2. An overall fit of the complete energy interval between 3.6 and 5.0 GeV seems unreasonable since the exact charm threshold behavior is not really known.

Table 2. Resonance parameters of the resonancelike regions between $4.0 \text{ GeV} < \sqrt{s} < 5.0 \text{ GeV}$

Mass (GeV/c ²)	Width (MeV/c ²)
4.04 ± 0.02	55 ± 10
4.15 ± 0.04	47 ± 11
4.40 ± 0.03	33 ± 9

Although within the systematic uncertainties our measurements are in overall agreement with other results, there are some differences. The PLUTO cross section is somewhat lower than that of the DASP⁽⁶⁾ and the SLAC-LBL⁽⁷⁾-detectors while it is in agreement with the preliminary cross section of the DELCO-detector⁽⁸⁾. The peaks at 4.04 GeV and at 4.15 GeV are well separated in the PLUTO and DASP results, but this is not so for DELCO and SLAC-LBL results.

4. ρ -inclusive Production

The quarks are assumed to be pointlike spin half constituents of hadrons. A meson h is built up by a quark-antiquark pair. So it is obvious from simple spin state counting that the vector mesons (spin $J = 1$) should be produced three times more frequent than the pseudoscalar-mesons ($J = 0$) in the inclusive reaction

$$e^+e^- \rightarrow h + \text{anything}.$$

(In this estimate more sophisticated items of the theory, like quark mass differences, are neglected). We compared our measurements of the inclusive reaction

$$e^+e^- \rightarrow \rho^0 + \text{anything} \quad (1a)$$

with

$$e^+e^- \rightarrow \pi^\pm + \text{anything}, \quad (1b)$$

taking ρ ($J = 1$) and π ($J = 0$) as the mesons with the smallest mass of each type to test this prediction. Reaction (1b) has been measured by the DASP-collaboration⁽⁹⁾. To look for events of the

reaction (1a) we assigned pion mass to all tracks and plotted the invariant mass of two tracks with opposite charge (fig.3a,upper histogram). The background was determined using pairs of tracks, each track coming from a different event (fig.3a,lower histogram).

The invariant masses of the remaining events have been plotted in fig.3b. The mass distribution has been fitted to the ρ^0 -resonance (giving mass and width of 767 ± 7 MeV and 160 ± 40 MeV respectively from a Breit-Wigner-fit), a smooth polynomial background and a possible kinematic reflection of $K^*(890)$ which contributes to the left tail of the ρ^0 -signal when the $K\bar{K}$ is interpreted as two pions.

The cross section of the reaction (1a) as a function of the center of mass energy \sqrt{s} is shown in fig.4 in terms of

$$R_\rho = \sigma(e^+e^- + \rho^0 + X)/\sigma_{\mu\mu} .$$

Like the total hadronic cross section the ρ^0 -inclusive cross section shows also a threshold behavior between $3.6 \text{ GeV} \leq \sqrt{s} \leq 4.1 \text{ GeV}$. Above $\sqrt{s} = 4.1 \text{ GeV}$ a value of $R_\rho \sim 1$ is obtained.

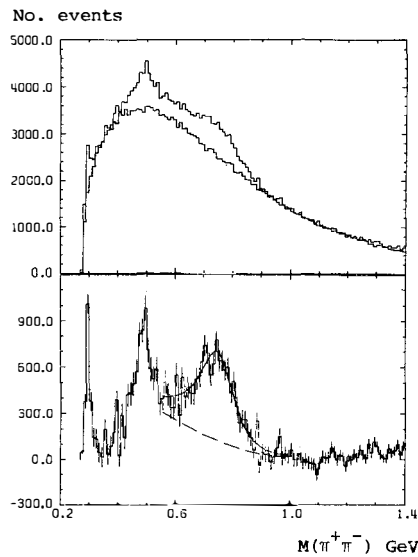


Fig.3 a) Invariant mass of $\pi^+\pi^-$ system (upper histogram) and uncorrelated pairs (lower histogram)
 b) Difference between correlated and uncorrelated $\pi^+\pi^-$ -pairs

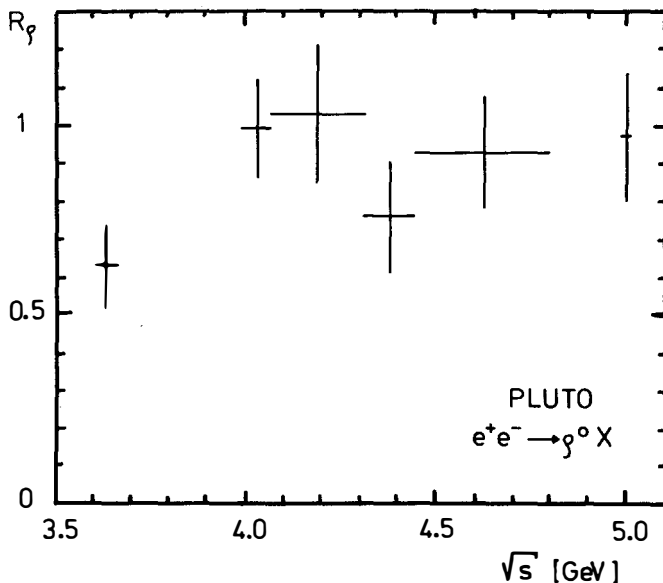


Fig.4. ρ^0 inclusive cross section normalised to the μ -pair cross section as a function of the center of mass energy \sqrt{s}

The energy distribution of the ρ can be written as

$$\frac{s}{\beta} \frac{d\sigma}{dx_E} = f(x_E, s)$$

with $x_E = 2 E_\rho / \sqrt{s}$, E_ρ = energy of the ρ , and β = velocity of the ρ . For high center of mass energies scaling predicts f to become only a function of x_E

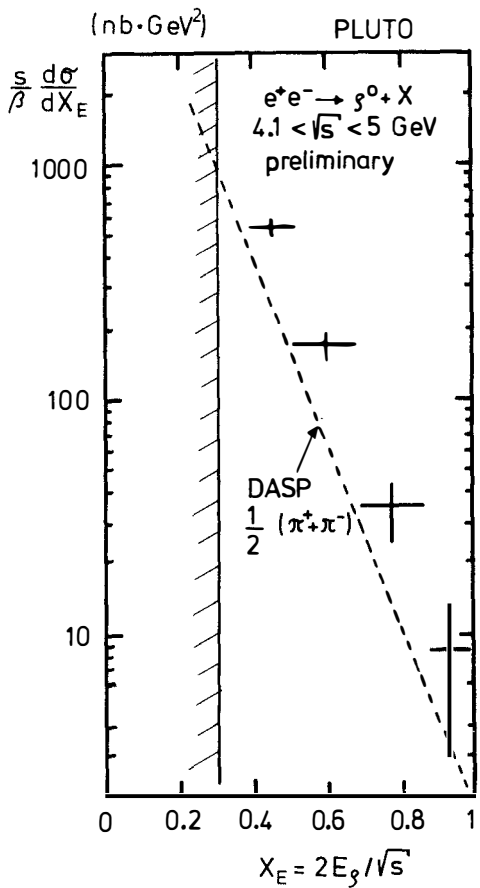
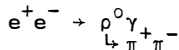


Fig.5. ρ^0 inclusive energy distribution. The broken line represents the DASP result for the charged pion inclusive reaction (1b). The full line is the kinematic limit at $x_E = 2m_\rho / \sqrt{s}$

one can calculate the fraction of pions from a ρ decay and can subtract them from the π -inclusive spectrum, obtaining a direct π spectrum.

The obtained spectrum is shown in fig.5. Due to the limited center of mass energy interval from 3.6 GeV to 5.0 GeV, in which data have been taken, there is a lower kinematical limit for x_E at ~ 0.3 . Events from the reaction



have been detected experimentally and removed as a background which contributes to the events in the $x_E \sim 1$ region. This reaction can be calculated from QED. The measured contribution is in agreement with this calculation.

The slope of the curve can be parameterized as

$$f_\rho(x_E) \propto \exp(-b \cdot x_E)$$

with $b = 8.4 \pm 0.8$ or as

$$f_\rho(x_E) \propto \frac{1}{x_E} \cdot (1-x_E)^n$$

$$\text{with } n = 2.4 \pm 0.4 .$$

The broken line in fig.5 represents the inclusive π production as measured by DASP. To compare the ρ -inclusive production, one must take into account that a certain number of observed pions are coming from the ρ -decay.

Assuming the cross section for all ρ to be

$$\sigma(\rho^+ + \rho^- + \rho^0) = 3 \cdot \sigma(\rho^0)$$

Comparing this spectrum with the measured ρ -inclusive spectrum one obtains for $x_E \geq 0.4$

$$\frac{(\frac{s}{\beta} \frac{d\sigma}{dx_E})_\rho}{(\frac{s}{\beta} \frac{d\sigma}{dx_E})_\pi \text{ direct}} = 3.1 \pm 0.6$$

in good agreement with expectation. However, this is an upper limit since there are also contributions to the π -direct-spectrum from other resonance decays.

5. The Radiative Decay $J/\psi \rightarrow f^0 \gamma$

Radiative decays of the J/ψ like

$$J/\psi \rightarrow \pi^0 \gamma \quad (2a)$$

$$J/\psi \rightarrow \eta \gamma \quad (2b)$$

$$J/\psi \rightarrow \eta' \gamma \quad (2c)$$

$$J/\psi \rightarrow f^0 \gamma \quad (2d)$$

are a useful tool to provide information on the mechanism of Zweig-rule violation. In the language of QCD radiative decays are described by two different types of graphs (fig.6)

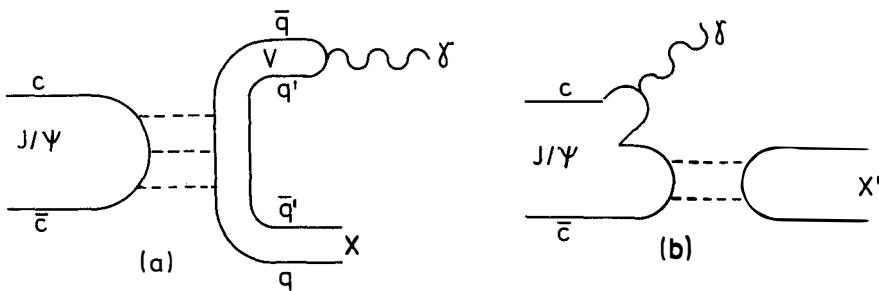


Fig.6 Diagrams for radiative decays via 3 gluon-(a) and 2 gluon-exchange (b)

In the first diagram (fig.6a) the decay is mediated by a three gluon coupling to an intermediate vectormeson V and a hadronic system X with a subsequent transition of V via vectordominance to a photon.

The calculation of this decay scheme leads to relatively small branching ratios. This has been found to be true for the decay (2a), indeed, the DASP-collaboration found

$$\text{BR}(J/\psi \rightarrow \pi^0 \gamma) = (7.3 \pm 4.7) \cdot 10^{-5} \quad (10)$$

But the branching ratios for decays (2b) and (2c) are considerably higher. The DASP- und DESY-Heidelberg-groups measured

$$\text{BR}(J/\psi \rightarrow \eta \gamma) = \begin{cases} (0.80 \pm 0.18) \cdot 10^{-3} & \text{DASP}^{(10)} \\ (1.3 \pm 0.4) \cdot 10^{-3} & \text{DESY-HD}^{(11)} \end{cases}$$

$$\text{BR}(J/\psi \rightarrow \eta' \gamma) = \begin{cases} (2.2 \pm 1.7) \cdot 10^{-3} & \text{DASP}^{(10)} \\ (2.4 \pm 0.7) \cdot 10^{-3} & \text{DESY-HD}^{(11)} \end{cases}$$

These branching ratios can be explained with the second graph (fig.6b), where the decay is mediated only by a two gluon exchange. The branching ratio into a photon and two gluons has been estimated to be

$$\text{BR}(J/\psi \rightarrow \gamma + 2 \text{ gluons}) \sim 10\%. \quad (12)$$

This leads to predictions that decays like (2b) and (2c) should have considerably higher branching ratios than reaction (2a). The decay (2a) cannot proceed via this graph (fig.6b) due to isospin conservation.

To provide more information it is worthwhile to study the decay (2d). In doing so, the PLUTO collaboration - as recently reported⁽¹³⁾ - selected from 84000 J/ψ events those with two prongs plus one photon. For the latter only the direction has been determined. 1650 events fit the hypothesis

$$J/\psi \rightarrow \pi^+ \pi^- \gamma \quad (3\text{-C-fit}).$$

After QED-background rejection we obtain a sample of 852 events which are either $\pi^+\pi^-\gamma$ or $\pi^+\pi^-\pi^0$ (with only one γ of the π^0 detected or both γ are not resolved).

The invariant mass distribution of the neutral combination $\pi^+\pi^-$ of events not lying in the ρ^\pm -band ($0.6 \text{ GeV}/c^2 \leq M(\pi^\pm\pi^0) \leq 1 \text{ GeV}/c^2$) shows two peaks (fig.7a). A fit gives two Breit-Wigner-resonances with masses of $(0.78 \pm 0.02) \text{ GeV}/c^2$ and $(1.23 \pm 0.04) \text{ GeV}/c^2$ and widths of $(0.13 \pm 0.02) \text{ GeV}/c^2$ and $(0.13 \pm 0.05) \text{ GeV}/c^2$ respectively, in agreement with the ρ^0 and the $f^0(1270)$ mesons. $\rho'(1250)$ could be excluded for the second peak, because the invariant mass distribution of the charged combination $(\pi^\pm + X, X = \gamma \text{ or } \pi^0)$ shows no adequate peak in this region (fig.7b) which is expected for the iso-spin triplet $\rho'(1250)$.

Charge conjugation implies that the ρ^0 is accompanied by a π^0 and the f^0 by a γ . Using our Monte-Carlo-procedure to determine the overall efficiency we obtained the following branching ratios:

$$\begin{aligned} BR(J/\psi \rightarrow \rho^0\pi^0) &= (1.6 \pm 0.4)\% \\ BR(J/\psi \rightarrow f^0\gamma) &= (0.2 \pm 0.07)\% \end{aligned}$$

The DASP-collaboration has obtained similar results ⁽¹⁴⁾. Due to the fact that the branching ratio for the decay (2d) is of the same order of magnitude as for the decays (2b) and (2c), one is urged to study this decay in the terms of the two-gluon-exchange diagram (fig.6b).

If one calculates this diagram, as done by M.Krammer ⁽¹⁵⁾, one obtains predictions for the angular distributions of the final state.

The decay (2d) is described by three independent f^0 -helicity amplitudes A_0 , A_1 and A_2 . The combined production- and decay-angular distribution for this reaction $W(\theta_p, \theta_M, \phi_M)$ is only a function of the ratios $A_1/A_0 = X$ and $A_2/A_0 = Y$, where θ_p is the angle between the f^0 direction and the e^+ -beam, θ_M and ϕ_M are polar and azimuthal angles of the π^+ in the f^0 helicity frame. X and Y may have values between plus and minus infinity in principle.

For a given pair of values X and Y we have fitted our data (after a background subtraction) to the angular distribution $W(\theta_p, \theta_M, \phi_M)$ comparing by χ^2 -values the distributions for different X and Y values. Details of this procedure will be published soon ⁽¹⁶⁾.

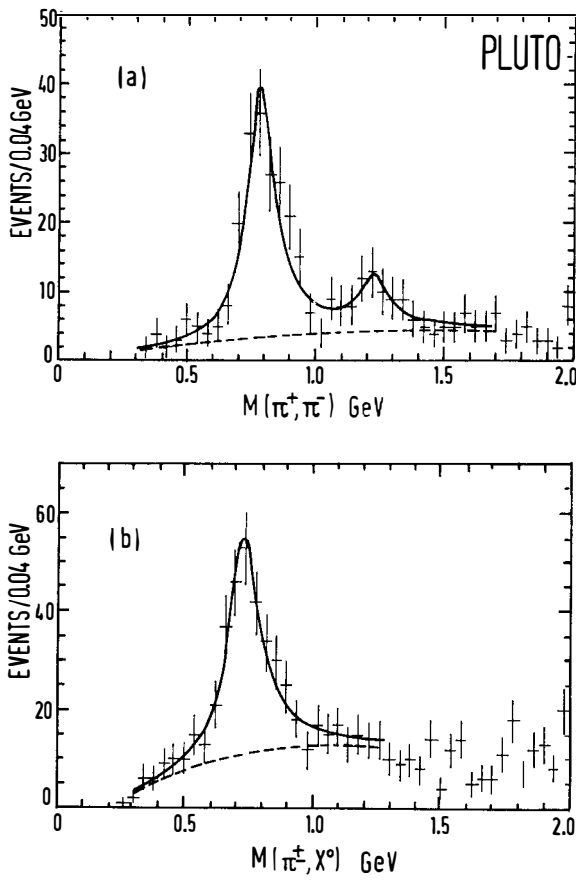
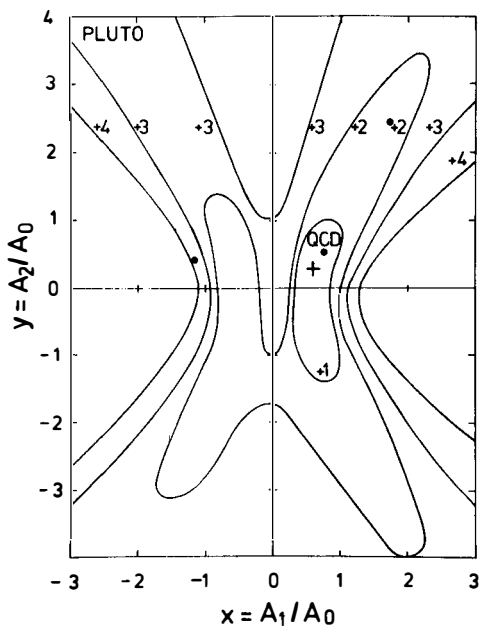


Fig.7. Invariant mass distributions
 a) Neutral combination ($\pi^+ \pi^-$), excluding events from
 the ρ -band
 b) Charged combination ($\pi^+ X^0$, $X^0 = \gamma$ or π^0)
 The full line gives the fit above an estimated polynomial
 background (dashed line)

The results of these fits are presented in fig.8 in form of equal χ^2 contours in the X-Y-plane. The χ^2 -values assigned to the curves are measured from the minimum of $\chi^2 = 26$ (25 degrees of freedom). The best values obtained in these fits are



$$X = A_1/A_0 = 0.6 \pm 0.3$$

$$Y = A_2/A_0 = 0.3^{+0.6}_{-1.6}$$

(crossed point in fig.8).

The values of $X = 0.76$ and $Y = 0.54$ as predicted by from the QCD-two-gluon-exchange⁽¹⁵⁾ are in very good agreement with our results.

Fig.8
Fit of the f_0 -decay distribution. Curves are representing equal χ^2 -values, measured from the minimum of $\chi^2=26$. QCD marks the prediction from the two gluon-exchange model

6. Heavy Lepton

6.1 Introduction

Just one year ago the existence of the heavy lepton, found in e^+e^- -annihilation in 1975 by the SLAC-LBL-collaboration ⁽¹⁷⁾, has been confirmed by the PLUTO-Collaboration ^(18,19). It should also be mentioned that M.Perl named this new particle τ ⁽²⁰⁾ at the Rencontre de Moriond one year ago.

During the last year a very fruitful work on this particle has been performed by several groups, but there are still some questions open.

The PLUTO collaboration can contribute new results on two of such subjects: we measured the branching ratio of the hadronic decay mode $\tau \rightarrow p\pi\nu$ and we can give an new upper limit on the lifetime of the τ .

Before going into the details of our measurements let me repeat some main properties of the τ . As discussed above, in the total hadronic cross section there is need to explain at least one unit of R_{tot} above the threshold around 3.6 GeV, which is assigned to the heavy lepton τ . From very accurate measurements of DASP ⁽²¹⁾ and DESY-Heidelberg ⁽²²⁾, we know that the mass of the τ is a few MeV less than 1.8 GeV, further we know that the τ behaves like a point-like spin half particle. In the decays of the τ a neutral particle is emitted, presumably a new neutrino ν_τ .

Therefore it is reasonable to discuss the properties of the τ in terms of a sequential (heavy) lepton, having its own (conserved) lepton number and thus its own neutrino (mass assumed to be zero). Using conventional weak current-current-interactions (with at least an arbitrary mixture of V and A components in the τ -part of the current), one can calculate the branching ratio into its simplest decay modes, as done e.g. by Thacker and Sakurai ⁽²³⁾. Using their formulae and taking into account recent measurements of the total hadronic cross section in the region below the mass of the τ , one obtains the branching ratios of table 3 ⁽²⁴⁾. The measured branching ratios for the purely leptonic decay modes are in good agreement with theory: the world's average value, as presented at the Hamburg Conference last summer ⁽²⁵⁾, is

$$BR(\tau \rightarrow e\nu\nu) = BR(\tau \rightarrow \mu\nu\nu) = (18+3) \%$$

Table 3 Branching ratios of the heavy lepton

Decay mode	Branching ratio in %
$\tau^- \rightarrow \nu_\tau e^- \bar{\nu}_e$	15.1
$\tau^- \rightarrow \nu_\tau \mu^- \bar{\nu}_\mu$	14.7
$\tau^- \rightarrow \nu_\tau \pi^-$	7.5
$\tau^- \rightarrow \nu_\tau \rho^-$	20.3
$\tau^- \rightarrow \nu_\tau + (\text{strange particles})$	1.9
$\tau^- \rightarrow \nu_\tau A_1^-$	7.8
$\tau^- \rightarrow \nu_\tau + (\text{hadr. continuum})$	32.7

But there are still some difficulties with some hadronic decay modes. The vector part of the weak hadronic current behaves as predicted. The branching ratio $\tau^- \rightarrow \nu_\tau \rho^-$ has been measured by the DASP-Collaboration to be in agreement with theory⁽²⁶⁾. But the axialvector part of the weak hadronic current should couple to the A_1 -meson as the lowest axialvector ($J^P = 1^+$) state and via the divergence of the current to the π as lowest pseudoscalar ($J^P = 0^-$) state. Especially the decay $\tau^- \rightarrow \nu_\tau \pi^-$ can be calculated, because it depends only on the pion coupling constant f_π , which is well known from the decay $\pi^- \rightarrow \mu^- \bar{\nu}_\mu$. The ratio should be

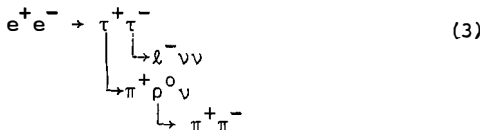
$$BR(\tau^- \rightarrow \nu_\tau \pi^-) / BR(\tau^- \rightarrow \nu_\tau e^- \bar{\nu}_e) = 0.5$$

but there is no positive evidence for this decay. The only measurement of the DASP^(26,27) detector is somewhat lower than the predicted branching ratio.

On the other hand the decay to the A_1 -meson is problematic because the A_1 is in the language of the Particle Data Group⁽²⁸⁾ a "not established resonance". But to test the axialvector part of the current it is sufficient to look for a $J^P = 1^+$ hadronic final state (e.g. $\tau^- \rightarrow \nu_\tau \rho^+$) avoiding discussions on the existence of the A_1 . If the branching ratio of this decay is of the order of magnitude as predicted it is a strong evidence for the normal behaviour of the axialvector current.

6.2 The Decay $\tau \rightarrow \nu \rho \pi^*$ *)

We looked for events with a final state containing an identified lepton ℓ^\pm (e^\pm or μ^\pm) and three prongs with missing energy and no photon in the detector according to the reaction



Our selection criteria have been:

For an electron we required a momentum $p_e > .4 \text{ GeV}/c$ and for a muon $p_\mu > 1 \text{ GeV}/c$, a missing mass $MM > .9 \text{ GeV}/c^2$ and the energy of the 3-pion-system not greater than the beam energy. A typical event is shown in fig.9. After these cuts our sample contained 66 events, 52 of them with an identified electron. Fig.10 shows the mass of the 3-pion-system versus the lepton momentum. There is no correlation between these two quantities as expected for reaction (3). The 3-pion-mass is distributed in a small band around $1.1 \text{ GeV}/c$.

Both the electron and the muon momentum spectra are relatively hard. Several checks have been made to assure that the observed events are really in agreement with reaction (3) (30). As an example I shall discuss here only the spectrum of electrons (fig.11, histogram). From the measured spectrum we subtracted the background from hadron - electron misidentification $p(h + e) = 1.2\%$, taking into account, that the electron detection efficiency is a function of the electron momentum,

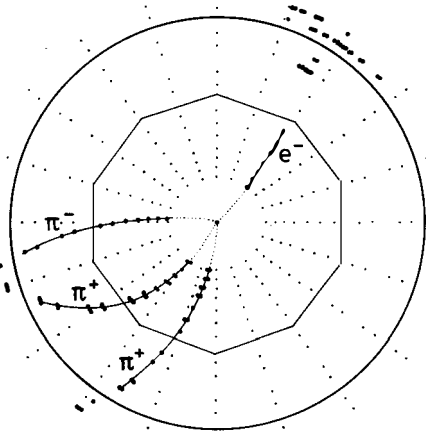


Fig.9. Typical event of reaction (3)
(view along the beam-line)

*) Results of this channel have recently been published by the PLUTO group (29). Meanwhile we doubled statistics lowering some cuts and taking also events with a muon instead of an electron.

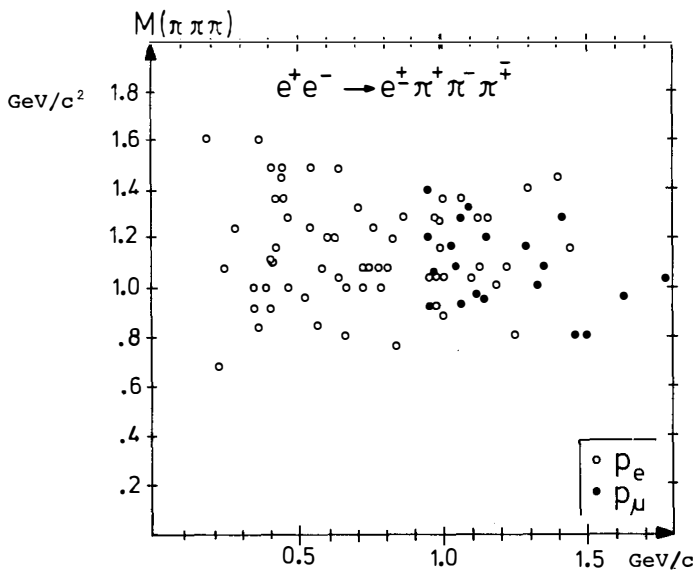


Fig.10. Mass of the 3-pion system versus lepton momentum.
Muons with momenta less than ~ 1 GeV/c are not recorded
due to the cut-off of the iron yoke

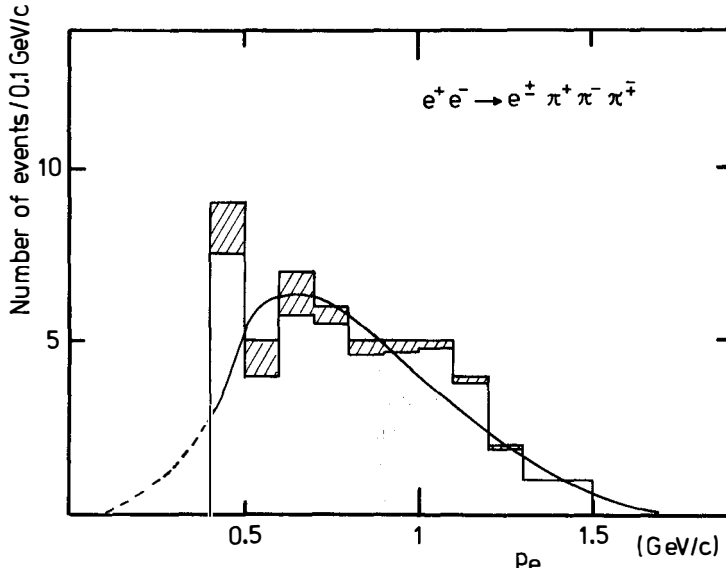


Fig.11 Measured spectrum of the electrons.
The hatched area represents background from hadron-electron
misidentification. The curve is the calculated electron spec-
trum of the τ decay folded with the electron detection
efficiency and normalized to the data.

which raises from 30% at $p_e = 0.4$ GeV/c to 65% at $p_e = 1.0$ GeV/c. In fig.11 the hatched area represents this background. The remaining electron spectrum is in good agreement with the theoretical electron spectrum from τ -decay (full line in fig.11).

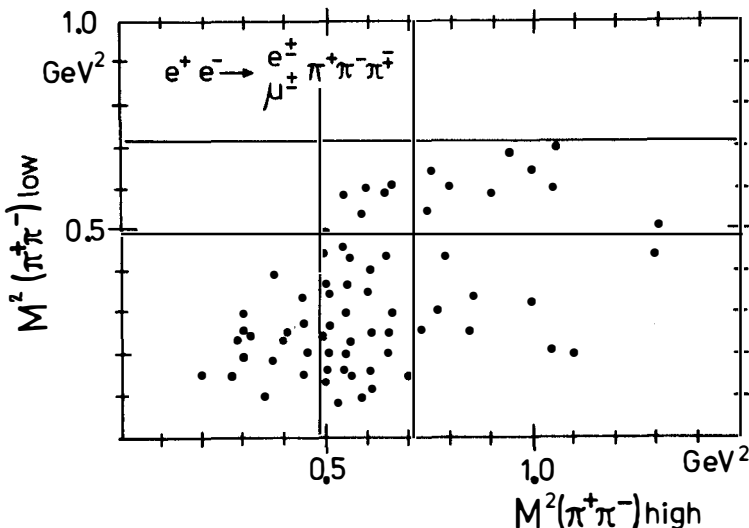


Fig.12. Low mass combination versus high mass combination of the 2-pion-system. The full lines at $.49 \text{ GeV}^2$ and at $.7 \text{ GeV}^2$ are representing the ρ^0 -cut applied to the data in further use.

The Dalitz plot (fig.12) shows a well populated ρ^0 -band. Thus we required for our further analysis at least one 2-pion-combination to have a mass in the ρ^0 -band i.e. $0.7 \text{ GeV}/c^2 \leq M(\pi^+\pi^-) \leq 0.84 \text{ GeV}/c^2$. After this cut 42 events (35 with an electron) remained in our analysis.

The background shows no ρ^0 -signal. Furthermore one can estimate the charm contribution to this channel to be less than 3 events. The momentum spectrum of the 3-pion-system is compatible with a two-body-decay of the τ which supports the interpretation of the $(\rho\pi)$ -system to be the A_1 resonance. Using our Monte-Carlo-procedure to determine all acceptances and efficiencies we obtained a branching ratio

$$\text{BR}(\tau^- \rightarrow \rho^0 \pi^- \nu) = (5 \pm 1.5) \%$$

or if one assumes an A_1 -resonance

$$BR(\tau^- \rightarrow \nu A_1^-) = (10 \pm 3) \%$$

From the 3-pion-mass-spectrum we derived further (under assumption of a two-body decay of the τ) an upper limit of the mass of the τ -neutrino $m_{\nu_\tau} < 4 \text{ GeV}/c^2$.

From the negative G-parity of the $(\rho\pi)$ -system one can conclude assuming conventional weak hadronic currents with V and A parts that the only allowed states have a spin-parity $J^P = 0^-$ or 1^+ . This is equivalent to the statement that the weak hadronic current must have an axialvector component.

If one admits non conventional weak interactions the lowest angular momentum states of the $(\rho\pi)$ -system are listed in table 4.

Table 4. Spin-Parity assignments of $(\rho\pi)$ -system
Assignments in brackets are only possible
in non conventional weak interactions.

λ	S	P	D
	0	1	2
$J = 0$		0^-	
		1^+	(1^-)
			(1^+)
$J = 1$			(2^-)
			(2^+)

In fig.13a the 3-pion-mass-spectrum, corrected for background and acceptance is compared with the S, P and D-wave solutions. No pure state gives an acceptable fit. The data fit best, if one uses the S-wave plus a Breit-Wigner-resonance with a mass of $1 \text{ GeV}/c^2$ and a width of 400 MeV , parameters which are in agreement with the A_1 resonance (fig.13b). Thus we conclude that the A_1 - if existing would give a good description of our data.

6.3 Upper limit of the Lifetime

From the standard model of a sequential heavy lepton with V-A decay structure the lifetime of the τ , τ_0 , is determined by

$$\tau_0 = BR(\tau \rightarrow e \bar{\nu} \nu) \cdot (M_\mu / M_\tau)^5 \cdot \tau_\mu$$

where τ_μ and M_μ are lifetime and mass of the muon. Using a branching ratio $BR(\tau \rightarrow e \bar{\nu} \nu) = 18 \%$ and a mass of the heavy lepton

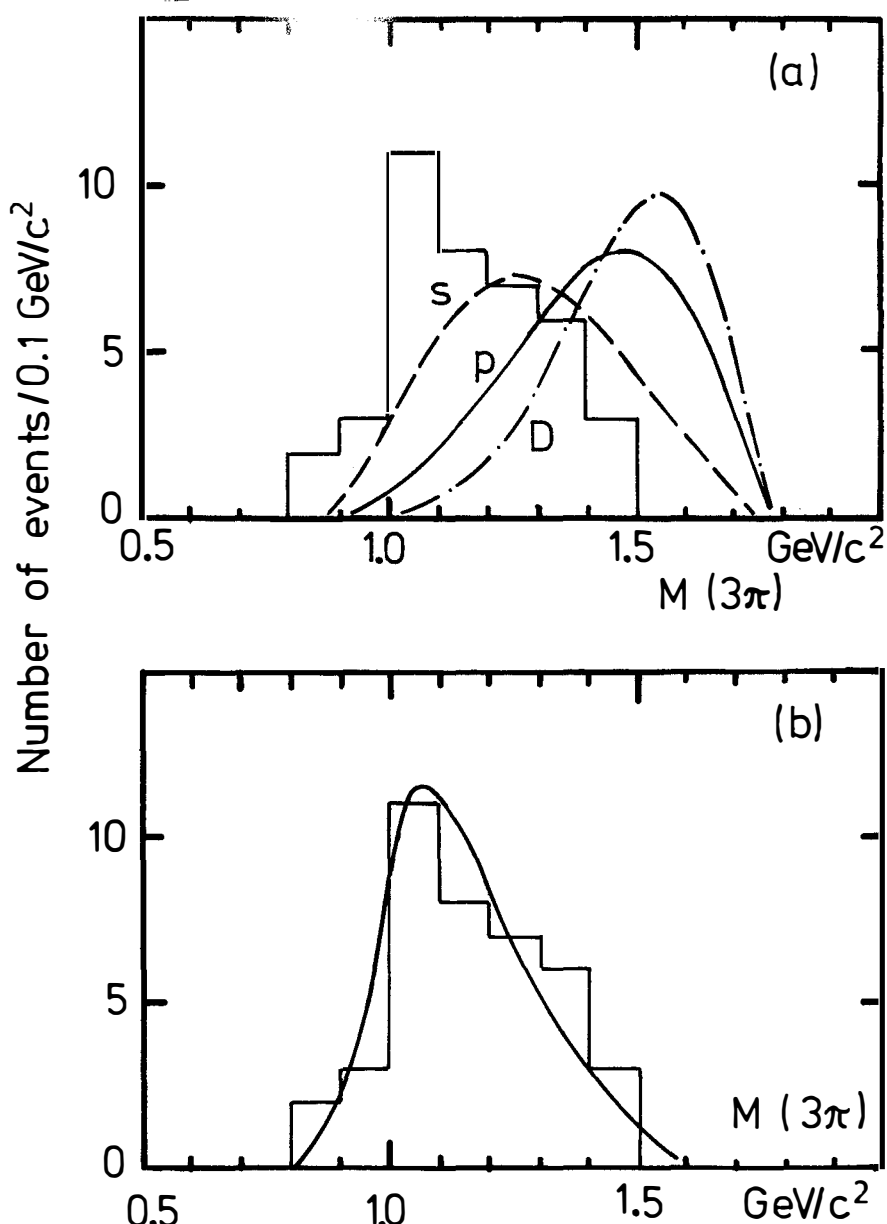


Fig.13 3-pion mass spectrum, corrected for background and acceptance (histogram) and
 a) theoretical distributions for S, P and D wave solutions
 b) theoretical distribution for a S-wave plus a Breit-Wigner resonance ($M = 1 \text{ GeV}/c^2$, $\Gamma = 400 \text{ MeV}/c^2$)

$M_\tau = 1795 \text{ MeV}/c^2$ one obtains

$$\tau_0 = 2.8 \cdot 10^{-13} \text{ sec.}$$

The lifetime can be determined by measuring the average decay length d_0 at a fixed momentum of the τ . But this length is far too small ($d_0 \sim 0.05 \text{ mm}$) to be determined by the PLUTO-detector.

For this analysis we used our $(e^+e^- \rightarrow \mu^\pm + 1 \text{ prong} + \text{no photon})$ event sample as used for our anomalous muon analysis (18) and applied some further cuts to get a sample of events which make a very accurate momentum measurement possible. Thus we required a missing mass $MM^2 > 0.4 E_{\text{beam}}^2$, a coplanarity angle $15^\circ < \Delta\phi < 165^\circ$, ≥ 10 coordinates for each track and a momentum for the non-muon track $p_2 > 0.4 \text{ GeV}/c$. In addition we used a special tracking procedure, taking into account the energy loss in the matter transversed by the particle.

Fig.14 shows the vertex-distribution from the remaining 65 events. For each track the minimal distance to the interaction point in the plane perpendicular to the beam (r_{\min}) has been determined and entered into the plot. The accuracy of the position of the interaction point in this plane is $\Delta x = 0.5 \text{ mm}$ and $\Delta y = 0.7 \text{ mm}$ (FWHM). The vertex-distribution fits well by a Gaussian with a $\sigma = 3.05 \pm 0.15 \text{ mm}$ (broken line in fig.14). To examine the influence of a finite decay length on the width of the vertex distribution we used our Monte-Carlo-procedure and generated events with different decay lengths. The result of this calculations is presented in fig. 15, showing σ of the vertex-distributions as a function of the decay length.

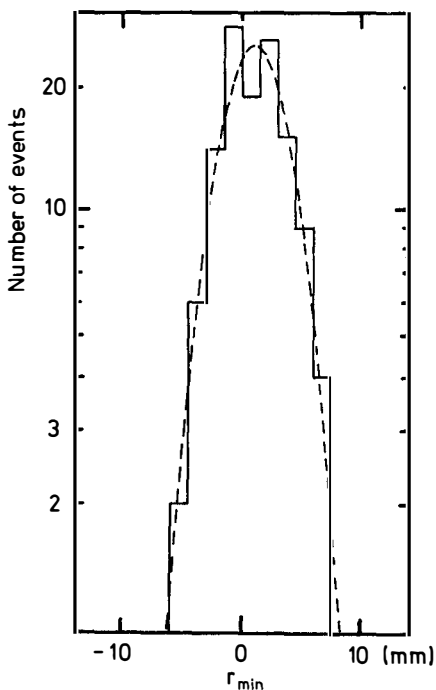


Fig.14 Vertex distribution in the plane perpendicular to the beam axis. The full line gives a fit to a Gaussian with $\sigma = (3.05 \pm 0.15) \text{ mm}$

The Monte-Carlo calculations show that the decay length distribution is compatible with the experimental resolution and therefore with a zero lifetime of the τ . Further we obtain from the calculation a two standard-deviation (95% C.L.) upper limit for the τ decay length $d_0 < 0.8$ mm, giving an upper limit on the lifetime of the

$$\tau_0 < 3.4 \cdot 10^{-12} \text{ sec. (95% C.L.)}$$

This upper limit excludes models of the heavy lepton predicting relatively long lifetimes (e.g. models mixing lepton numbers (31), predicting a lifetime of about 10^{-11} sec).

Since the lifetime is a very important parameter for testing theories, and unfortunately none of the existing experiments is sensitive enough to measure τ_0 , it might be worthwhile to design a detector specially for this purpose.

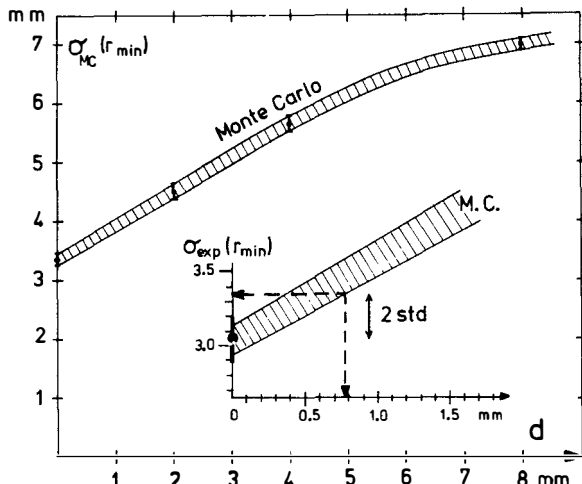


Fig.15. Width of the vertex distribution as a function of decay length obtained with a Monte-Carlo-procedure. In the insert the Monte-Carlo function is scaled down to the experimental value to derive the 2- σ - upper limit.

7. Present and Future Program of the PLUTO-detector

During the last year PLUTO was upgraded by installing a new system of shower counters of the lead-scintillator-sandwich type, covering a solid angle of 92% of 4π . The lead converters, shown in fig.1, have been removed. The new shower counters are equipped with proportional chambers to determine the position of the shower.

In addition, the muon detector has been enlarged and covers now 65% of the full solid angle.

During the same time the DORIS-storage ring has been upgraded to reach energies of more than 3.0 GeV per beam. It was operated from December 77 to February 78 at an energy of about 4 GeV per beam in single ring single bunch mode. During the time of this conference the energy will again be increased to reach a center of mass energy of 9.5 GeV to measure the T-resonance in e^+e^- annihilation. This resonance, recently found at Fermilab⁽³²⁾, is supposed to be a bound state of a new quark-antiquark pair. The resonance energy will be reached mid April. After a short runperiod of five weeks at the T-energy region PLUTO is scheduled to move to the new large e^+e^- -storage ring PETRA at DESY which will come into operation next autumn.

Note added after the conference

The DORIS-storage ring reached the energy of 9.2 GeV in schedule. An energy scan between 9.35 and 9.5 GeV center of mass energy was performed. PLUTO found the T-resonance at a mass of $(9.46 \pm 0.01)\text{GeV}/c^2$ (fig.16). The observed width of the resonance is compatible with the expected energy resolution of the storage ring. Thus we conclude, that the T is a narrow resonance being in agreement with the hypothesis of a bound state of a new quark-antiquark pair. From the value of the peak integral we further derive after applying radiative corrections an electronic width of the resonance of $(1.3 \pm 0.4)\text{keV}$, which favours a $-1/3$ charge assignment of the new quark⁽³³⁾.

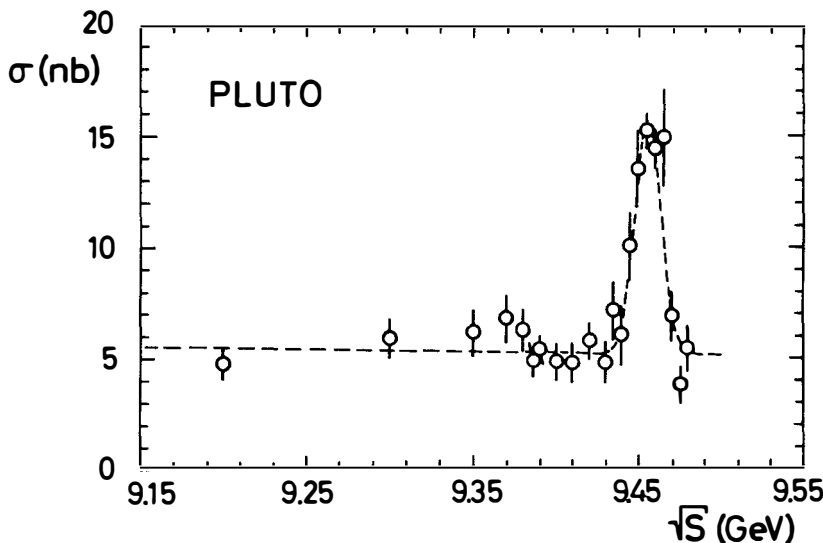


Fig.16. The total hadronic cross section in the T-resonance region in e^+e^- -annihilation (without radiative corrections). Only statistical errors are shown. The broken line gives a gaussian fit to the resonance curve with a $1/s$ hadronic background.

Acknowledgements

I wish to thank all my colleagues from the PLUTO-collaboration for their active help in preparing this talk, namely Prof.C.Grupen, Dr.G.Flügge, Prof.H.Meyer and Prof.G.Zech for many useful discussions. Further I like to thank the DESY directorate for their kind hospitality.

This work was supported by the Bundesministerium für Forschung und Technologie.

References

1. V.Blobel, in Proceedings of the XII Rencontre de Moriond (J.Tran Thanh Van, ed.), Paris 1977, Vol.I, p.99
2. PLUTO-collaboration, J.Burmester et al., Phys.Lett. 64B (1976) 369
3. PLUTO-collaboration, J.Burmester et al., Phys.Lett. 66B (1977) 395
4. G.Knies, in Proceedings of the 1977 Intern.Symp.on Lepton and Photon Interactions (F.Gutbrod, ed.), Hamburg 1977, p.93
5. A.Bäcker, Ph.D. thesis, Siegen Univ.(1977), DESY-internal report F33-77/03 (unpublished)
6. DASP-collaboration, R.Brandelik et al., DESY-report 78/18(1978)
7. G. Hanson, this conference
8. J.Kirkby, Proceedings of the 1977 Intern.Symp.on Lepton and Photon Interactions (F.Gutbrod, ed.) Hamburg 1977, p.3; A.Diamant-Berger, this conference
9. DASP collaboration, R.Brandelik et al., Phys.Lett. 67B (1977) 358
10. DASP collaboration, W.Braunschweig et al., Phys.Lett. 67B (1977) 243
11. DESY-Heidelberg-collaboration, W.Bartel et al., Phys.Lett. 66B (1977) 489
12. T.Appelquist et al., Phys.Rev.Lett. 34 (1975) 365, M.Chanowitz, Phys.Rev.D 12 (1975) 918, L.Okun and M.Voloshin, Moscow 1976, IETF-95
13. PLUTO-collaboration, G.Alexander et al., Phys.Lett. 72B (1978) 493
14. DASP-collaboration, R.Brandelik et al., Phys.Lett. 74B (1978) 292
15. M.Krammer, DESY report 78/06 (1978) and this conference
16. PLUTO-collaboration, G.Alexander et al., DESY report 78/20 (1978) (to be published in Phys.Lett.B.)
17. M.Perl et al., Phys.Rev.Lett. 35 (1975) 1489
18. PLUTO-collaboration, J.Burmester et al., Phys.Lett. 68B (1977) 297
19. PLUTO-collaboration, J.Burmester et al., Phys.Lett. 68B (1977) 301
20. M.Perl, in Proceedings of the XII Rencontre de Moriond (J.Tran Thanh Van, ed.), Paris 1977, Vol.I, p.75
21. DASP-collaboration, R.Brandelik et al., Phys.Lett. 73B (1978) 109
22. DESY Heidelberg-collaboration., P.Steffen, talk at the "Frühjahrstagung der DPG" at Heidelberg (1978)
23. H.B.Thacker and J.J.Sakurai, Phys.Lett. 36B (1971) 103
24. M.Rößler, Ph.D.thesis, Hamburg Univ.1978, DESY internal report F14-78/01 (unpublished)
25. E.Lohrmann, in Proceedings of the 1977 Intern.Symp.on Lepton and Photon Interactions (F.Gutbrod, ed.), Hamburg 1977, p.641
26. S.Yamada, in Proceedings of the 1977 Intern.Symp.on Lepton and Photon Interactions (F.Gutbrod,ed.), Hamburg 1977, p.69
27. G.Wolf, this conference

28. Particle Data Group, N.Barash-Schmidt, Rev.Mod.Phys.48,No.2, Part II (1976)
29. PLUTO-collaboration, G.Alexander et al.,Phys.Lett.73B(1978)99
30. W.Wagner, Ph.D.thesis, Aachen Univ.(1978) (unpublished)
31. H.Fritsch, Phys.Lett.67B (1977) 451
32. W.Herb et al.,Phys.Rev.Lett. 39 (1977) 252; L.Lederman, this conference
33. PLUTO-collaboration, Ch.Berger et al.,DESY report 78/21 (1978) (to be published in Phys.Lett.B)